Data Supplement for Yip et al.,Connectome-Based Prediction of Cocaine Abstinence. Am J Psychiatry (doi: 10.1176/appi.ajp.2018.17101147)

Data acquisition

Functional data were acquired on a Siemens Trio 3T scanner (Siemens AG, Erlangen, Germany) using a T2*-sensitive echo-planar image (EPI) gradient-echo pulse sequence (repetition time/echo time (TR/TE)=1500/27ms, flip angle=60º, field of view (FOV)=220x220mm, matrix=64x64, 3.4x3.4mm in-plane resolution, slice thickness=4mm with 1mm skip, 5mm effective slice thickness, 25 slices). High-resolution structural data were acquired using a sagittal high-resolution T1-weighted 3D magnetization-prepared-rapid-gradient-echo (MPRAGE) sequence (TR/TE=2530/3.34/2.77ms, flip angle=7º, FOV=256mm x 256mm, matrix=256x256, 176 slices, $1mm^3$ isotropic voxels).

Monetary incentive delay (MID) task description

A schematic diagram of the MID task(1) is shown in Supplemental Figure 1. During task performance, participants were presented with one of six cues (win \$1/\$0/\$5, lose \$0/\$1/\$5) for 1000ms, indicating the amount of money to be won or lost on that trial, followed by a fixation cross (variable delay). Participants were then presented with a target stimulus for a variable duration (individually calibrated based on out-of-scanner performance). To win (or avoid losing) the amount of money indicated by the cue, participants had to respond with a single button press while the target was on the screen. Following the target stimulus, a fixation cross was again presented, followed by feedback on the outcome of the trial (e.g., won \$1; did not lose \$5). Each MID run was approximately 12 minutes (22 win trials, 22 loss trials, 11 neutral trials). Participants completed two runs during scanning.

FIGURE S1. MID task design

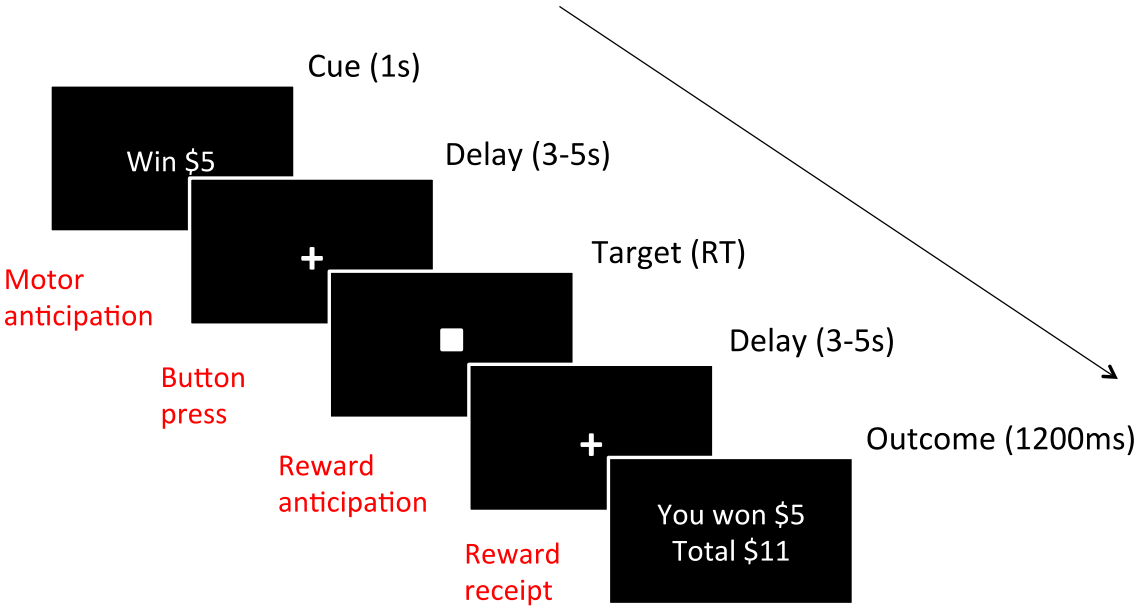

Pre-processing

The first six volumes of each functional run were discarded to allow for the magnetization to reach a steady state. Slice-time and motion correction was performed using SPM8 (http://www.fil.ion.ucl.ac.uk/spm/). All further analyses were performed using BioImage Suite(2). Several covariates of no interest were regressed from the data including linear and quadratic drifts, mean cerebral-spinal-fluid (CSF) signal, mean white-matter signal, and mean gray-matter signal. For additional control of possible motion-related confounds, a 24-parameter motion model (including six rigid-body motion parameters, six temporal derivatives, and these terms squared) was regressed from the data(3). The data were temporally smoothed with a Gaussian filter (approximate cutoff frequency=0.12Hz). Finally, for each participant, MID task runs were variance normalized and concatenated.

FIGURE S2. Schematic diagram of CPM applied to prediction of within-treatment abstinence

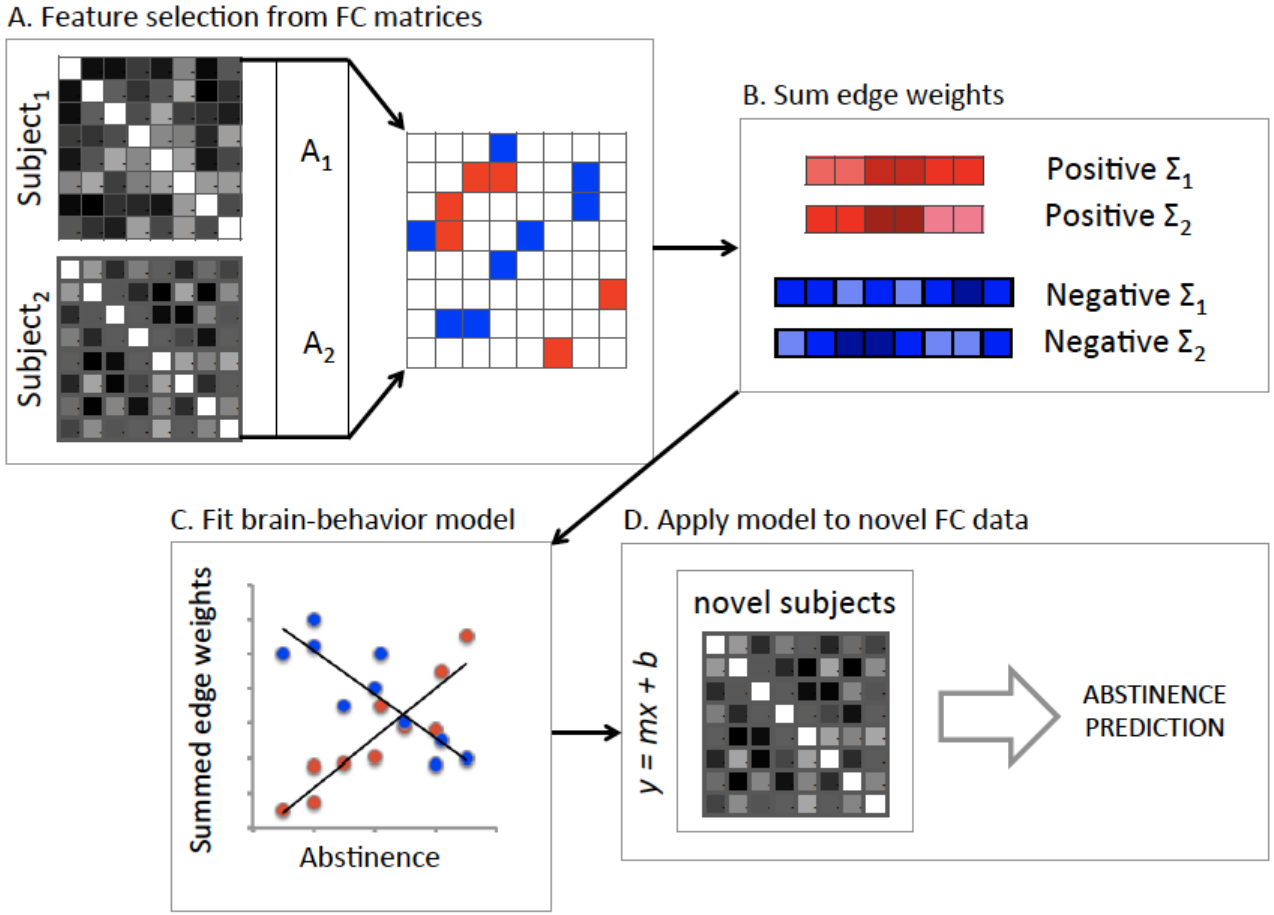

During CPM, 2A, edges (correlations between nodes in functional connectivity matrix) and behavioral data (cocaine negative urines) from a training dataset are correlated using regression analyses to identify positive and negative predictive networks (networks not shown). Single-subject summary statistics, 2B, are created as the sum of the edge weights in each network and, 2C, used to create predictive models assuming linear relationships with behavioral data. Resultant polynomial coefficients are applied to novel subject's FC matrices (2D, test data) to generate behavioral predictions. Model performance is evaluated based on the correlation between actual and predicted abstinence.

Network anatomy

Networks identified using CPM (and other predictive modeling approaches based on whole-brain connectomes) are typically complex and may be composed of multiple adjacent and nonadjacent nodes with varying degrees of connectivity (i.e., high- versus low-degree nodes). Thus, prior studies have summarized CPM networks using parcellation of network nodes either by spatial overlap with macroscale brain regions (e.g., prefrontal cortex, cerebellum) and/or by overlap with canonical networks (e.g., frontoparietal, motor/sensory; Supplemental Figure 3) (4-6). Here, we employ these standard approaches and summarize networks based on length-of-connection (short- versus long-range connectivity). Euclidean distance between the centroids of each brain region in the Shen atlas was used to classify short and long-range edges. First, distance was calculated for each pair of regions as: $\sqrt{((x_0 - x_1)^2 + (y_o - y_1)^2 + (z_0 - z_1)^2)}$, where (x_0, y_0, z_0), and $(x_1 y_1, z_1)$ represent the centroid for any two regions. Pair-wise distances were median separated into short and long-range connections.

Behavior-based prediction

To determine whether a combination of clinical features might also predict treatment response, we ran support vector regression (SVR) in MATLAB including baseline clinical variables (sex, age, pretreatment cocaine-use, pretreatment opioid-use, pretreatment alcohol-use, pretreatment cannabis-use, pretreatment cigarette-use, number of prior inpatient treatments, number of prior outpatient treatments, years of cocaine-use). SVR was run with permutation testing. To generate null distributions for significance testing, we randomly shuffled the correspondence between behavior variables and within-treatment abstinence 1,000 times and re-ran the SVR analysis with the shuffled data. Based on these null

distributions, p-values were calculated. SVR did not predict within treatment abstinence (r=0.08,p=0.25).

Motion controls

Task runs with excessive motion (>.30mm mean frame-to-frame displacement) were excluded. As described in the main manuscript, 17 individuals were excluded due to excessive motion, for a final sample of 53 individuals with 1 ≥ acceptable task runs (7 with one run and 45 with two runs). All subsequent CPM analyses were conducted with and without motion as an additional covariate, to test for putative effects of inter-individual variability in within-scanner motion on the variables of interest (abstinence and functional connectivity). As a further check of possible motion effects, participants were divided into 'high motion' and 'low motion' groups, as in prior CPM work (7), for post-hoc analyses (details below). 'High motion' was defined as >.20mm frame-to-frame displacement (n=19).

Overlap between networks identified with and without motion controls

CPM analyses not including motion as a covariate also successfully predicted abstinence (r's>.45, p's<0.002). Without motion as a covariate, the positive network included 400 unique edges. With motion as a covariate, the positive network included 266 edges (217 of which overlapped with the initial positive network; 81.6% overlap). Without motion as a covariate, the negative network included 447 unique edges. With motion as a covariate, the negative network included 263 edges (230 of which overlapped with the initial positive network; 86.5% overlap).

'High motion' and 'low motion' groups

As an additional control for motion effects, we divided participants into 'high' (n=19) and 'low' (n=34) motion groups ('high motion' defined as >.20mm frame-to-frame

displacement) and compared edge strength for positive and negative networks. If the edge selection step of the CPM analysis was driven by motion effects, then 'high motion' versus 'low motion' groups should significantly differ in edge strength(7). However, 'high motion' and 'low motion' groups did not differ in edge strength for positive ($F_{(2,52)}$=0.33, p=0. 571) or negative networks ($F_{(2,52)}$=0.76, p=0. 387).

Shen atlas registration

The 268-node atlas was warped from MNI space into single-subject space via concatenation of a series of linear and non-linear registrations between the functional images, MPRAGE scans, and the MNI brain. All transformation pairs were calculated independently, combined into a single transform, and inverted, warping the functional atlas into single participant space. This single transformation reduces interpolation error because the functional atlas is warped to an individual with only one transformation.

Follow-up analyses related to clinical variables

Given ethical concerns related to delaying treatment, the timing of fMRI scanning with respect to treatment initiation varied somewhat across individuals, with scans either occurring prior to treatment or within the first two weeks of treatment. On average, participants were scanned 1.9 days into the 84-day treatment period. Findings from follow-up analyses control for the effects of additional clinical variables are shown in Supplementary Table 1 (below).

Follow-up analyses related to other abstinence measures

Follow-up analyses confirmed significant relationships between self-reported abstinence (as defined via the Timeline Follow-back method) during treatment (percent days of self-reported abstinence: positive network: $r_{(df=52)}$=0.467, p<0.001; negative network:

$r_{(df=52)}$=-0.488, p<0.001; maximum days of consecutive abstinence: positive network: $r_{(df=52)}$=0.471, p<0.001; negative network: $r_{(df=52)}$=-0.486 p<0.001).

FIGURE S3. Canonical neural networks

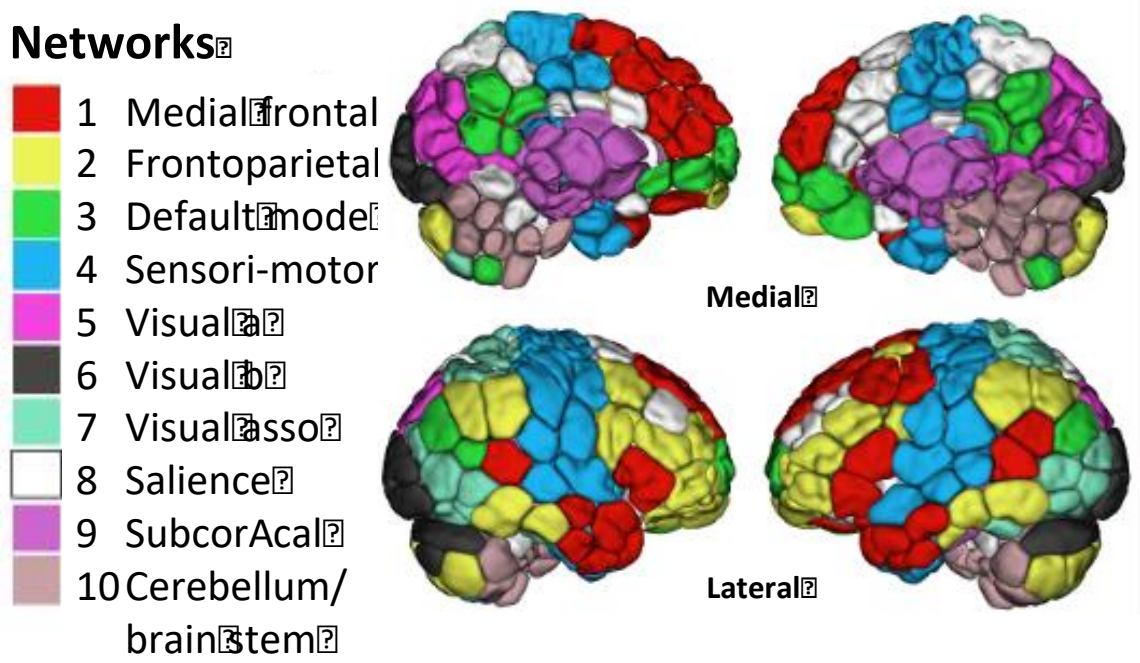

TABLE S1. CPM analyses controlling for clinical variables

	Positive		Negative		Both	
	R	P	R	P	R	p
Medication group	0.402	0.003	0.435	0.001	0.420	<.001
Methadone dose	0.435	0.003	0.451	0.001	0.457	0.001
Past month cocaine-use	0.428	0.004	0.449	0.001	0.459	0.001
Years of cocaine-use	0.416	0.003	0.426	0.001	0.426	0.002
Past month alcohol-use	0.450	<.001	0.456	<.001	0.457	<.001
Past month cannabis-use	0.449	0.002	0.457	<.001	0.461	<.001
Tobacco-use	0.435	0.001	0.466	<.001	0.455	<.001
Days in treatment	0.436	0.003	0.436	0.001	0.446	0.001
Timing of MRI scan	0.447	0.002	0.458	0.001	0.456	0.001

FIGURE S4. ROC curve for binary prediction in replication sample

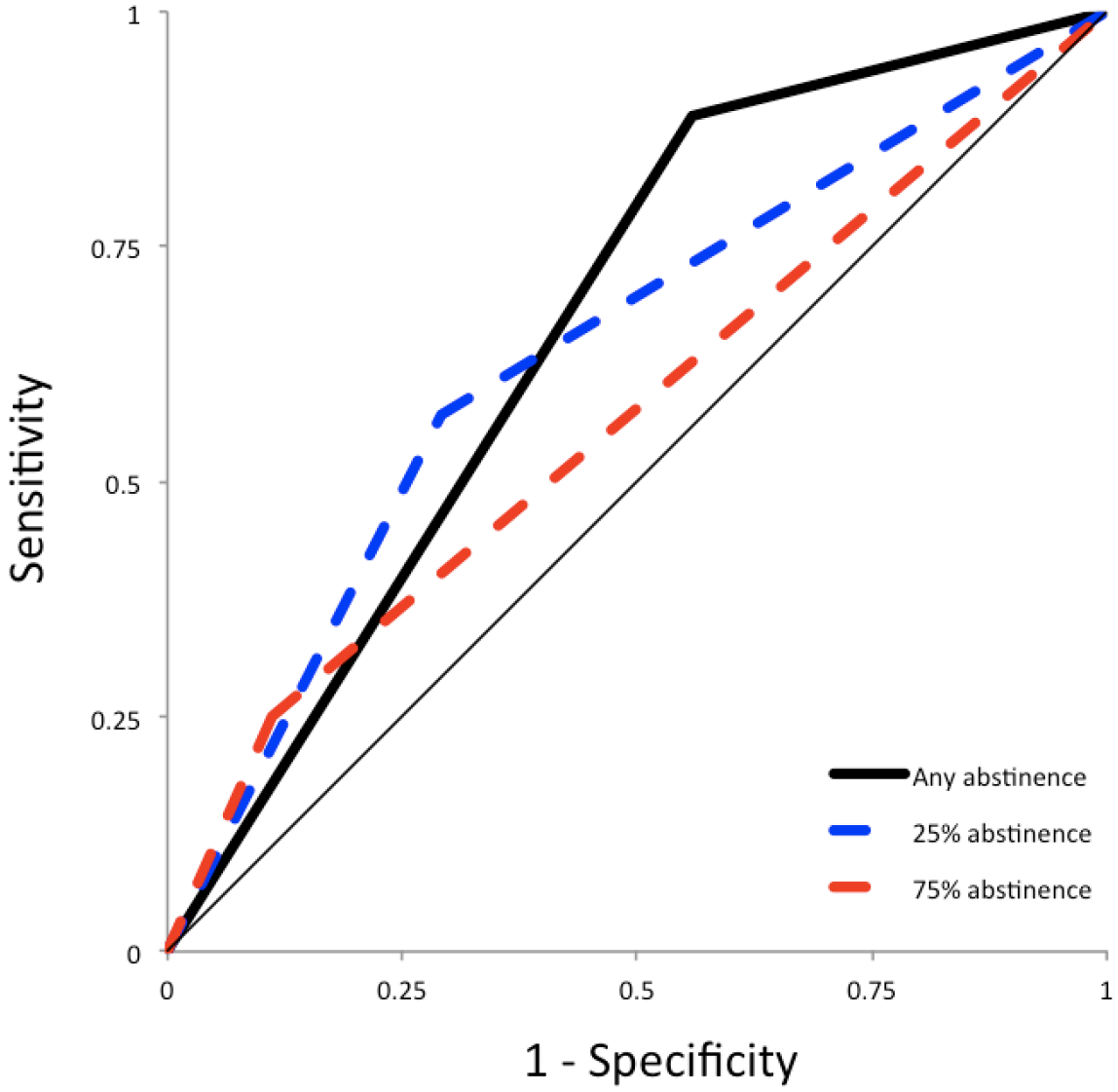

Solid black line represents ROC curve for network prediction of >0% drug free urines. Dashed blue line represents ROC curve for network prediction of ≥ 25% drug free urines. Dashed red line represents ROC curve for network prediction of ≥ 75% drug free urines. For reference, chance is plotted in grey. Baseline cocaine use is included in the model as a covariate.

References

1. Andrews MM, Meda SA, Thomas AD, Potenza MN, Krystal JH, Worhunsky P, Stevens MC, O'Malley S, Book GA, Reynolds B, Pearlson GD: Individuals Family History Positive for Alcoholism Show Functional Magnetic Resonance Imaging Differences in Reward Sensitivity That Are Related to Impulsivity Factors. Biol Psychiatry. 2011;69:675-683.
2. Joshi A, Scheinost D, Okuda H, Belhachemi D, Murphy I, Staib LH, Papademetris X: Unified framework for development, deployment and robust testing of neuroimaging algorithms. Neuroinformatics. 2011;9:69-84.
3. Satterthwaite TD, Elliott MA, Gerraty RT, Ruparel K, Loughead J, Calkins ME, Eickhoff SB, Hakonarson H, Gur RC, Gur RE, Wolf DH: An improved framework for confound regression and filtering for control of motion artifact in the preprocessing of resting-state functional connectivity data. Neuroimage. 2013;64:240-256.
4. Rosenberg MD, Finn ES, Scheinost D, Papademetris X, Shen X, Constable RT, Chun MM: A neuromarker of sustained attention from whole-brain functional connectivity. Nat Neurosci. 2016;19:165-171.
5. Finn ES, Shen X, Scheinost D, Rosenberg MD, Huang J, Chun MM, Papademetris X, Constable RT: Functional connectome fingerprinting: identifying individuals using patterns of brain connectivity. Nat Neurosci. 2015.
6. Noble S, Spann M, Tokoglu F, Shen X, Constable R, Scheinost D: Influences on the test-retest reliability of functional connectivity MRI and its relationship with behavioral utility. Cereb Cortex. 2017;27:5415-5429.
7. Rosenberg MD, Zhang S, Hsu WT, Scheinost D, Finn ES, Shen X, Constable RT, Li CS, Chun MM: Methylphenidate Modulates Functional Network Connectivity to Enhance Attention. J Neurosci. 2016;36:9547-9557.